Static and dynamic lateral deflexion of piles in non-homogeneous soil stratum

R. KRISHNAN*, G. GAZETAS* and A. VELEZ*

The Paper presents the results of a systematic parametric investigation of the static and dynamic response of single free-head piles embedded in a soil stratum, the modulus of which increases linearly with depth. The study is conducted by means of a dynamic finite-element formulation which accounts for the three-dimensionality of soil deformation while properly reproducing the radiation damping characteristics of the system. The soil is modelled as a linear hysteretic continuum and the excitation consists of a sinusoidally time-varying horizontal force or moment, applied at the pile head. Comprehensive plots of the results are presented in non-dimensional form, for a wide range of the most significant dimensionless groups of problem parameters. For the response of flexible piles, in particular, simple algebraic expressions are developed in terms of the ratio E_p/E_s, of the pile and soil moduli. These expressions, being valid for several values of Poisson's ratios of the soil, compare favourably with results from previous studies and are expected to be useful in practical design calculations.

Cet article donne les résultats de recherches paramétriques systématiques sur la réponse statique et dynamique des pieux libres en tête encastrés dans une couche de sol dont le module s'accroît linéairement avec la profondeur. L'étude est basée sur une formulation d'éléments finis dynamiques qui tient compte de la nature tridimensionelle de la déformation du sol, en même temps qu'elle reproduit de façon correcte les caractéristiques d'amortissement du système. Le sol est modelisé comme un continuum avec hystérésise linéaire et l'excitation consiste en une force horizontale qui varie de façon sinusoidale dans le temps appliquée en tête du pieu. Les résultats sont tracés de manière compréhensive sous une forme non-dimensionnelle pour une grande variété des groupes les plus importants des paramètres sans dimensions caractérisant le problème. Plus particulièrement pour la réponse des pieux flexibles des expressions simples algébriques sont présentées en fonction du rapport E_p/E_s des modules du pieu et du sol. Ces expressions, qui sont valables pour plusieurs valeurs du coefficient de Poisson pour le sol sont supérieures à celles fournies par les etudes précédentes, et on s'attend à ce qu'elles soient utiles pour les calculs pratiques des projects de fondations.

INTRODUCTION

Designing pile foundations to resist lateral loads, such as those arising from wind action, earth or water pressures, ocean waves, machines and earthquakes, primarily requires limiting the maximum pile deflexion to small values, acceptable for the safe operation of the superstructure. By contrast, ultimate lateral capacity is rather rarely the basis of design criteria for pile foundations. Consequently, careful engineering analysis of lateral pile deformations under the anticipated static or dynamic working loads is a crucial step to a satisfactory foundation design.

Some years ago, the design of piles against static lateral loads was based exclusively on empirical procedure developed from the results of full-scale tests. In more recent years, however, great engineering interest in the subject has led to the development of theoretical and semi-theoretical approaches for predicting static lateral deflexions of piles. One may broadly classify these approaches into three categories

(a) The 'beam on Winkler-foundation' approach which ignores the continuous nature of soil and simulates its lateral resistance against the pile through a set of independent, linear or non-linear, distributed 'springs' (Matlock & Reese, 1960; Matlock, 1970; and many others).

(b) The elastic continuum-type formulations which involve integration (direct or through boundary-element type discretizations) of the Mindlin (1936) equations for displacements due to a subsurface point load acting within a halfspace (Poulos, 1971a, 1971b; Banerjee & Davies, 1978).

(c) The finite-element formulations which invariably discretize both the pile and the surrounding soil into axisymmetric elements and rigorously enforce the boundary conditions at the pile–soil interface (Wittke, 1974; Randolph, 1981; Kuhlemeyer, 1979).

In addition to a number of formulations and computer programs which have been developed, numerous parametric studies have been published and solutions are now available in the form of non-dimensional graphs. From these graphs one can readily estimate the deflexion of end-bearing or

---

NOTATION

a_s dimensionless frequency factor ($= \omega d/V_s$)

$a_{s,n}$ frequency factor corresponding to the nth natural frequency of the soil stratum in vertically propagating shear waves

d pile diameter

E_p Young's modulus of pile

E Young's modulus of soil ($= E_s z/d$)

E_s Young's modulus of soil at depth $z = d$

f frequency of excitation (Hz)

G_s, V_s shear modulus and shear wave velocity of soil at depth $z = d$; $V_s = \sqrt{(G_s/\rho_s)}$

H thickness of the soil stratum

i $\sqrt{-1}$

I_{HH}, I_{HM} $= I_{MH}, I_{MM}$ imaginary parts of the normalized displacement factors U_{HH}, U_{MH}, U_{MM}

L pile length

l_s effective length of pile under static loading conditions

l_d effective length of pile under dynamic loading conditions

P, M horizontal force and moment applied at the pile head

R_{HH}, R_{HM} $= R_{MH}, R_{MM}$ real parts of the normalized displacement factors U_{HH}, U_{HM}, U_{MM}

t time

$u(z)$ lateral deflexion of the pile, function of depth z

U_{HH}, U_{MH} $= U_{HM}, U_{MM}$ normalized displacement factors relating pile-head motion to applied force and moment (equation (5))

$U_{HH}(z), U_{MH}(z),$ $U_{HM}(z), U_{MM}(z)$ displacement factors relating pile motion at a depth z to applied force and moment at the top

z depth below the ground surface

$\bar{z}_{HH}, \bar{z}_{HM}, \bar{z}_{MM}$ depths used for determining moduli of statically equivalent homogeneous deposits

β hysteretic damping ratio of soil

λ_s wavelength of shear waves corresponding to a depth $z = d$ ($\lambda_s = V_s/f$)

v Poisson's ratio of soil

$\theta(z)$ rotation of the pile, function of depth z ($= \mathrm{d}u(z)/\mathrm{d}z$)

ρ_s, ρ_p mass density of soil and pile

ω circular frequency of vibration in rad/s

ω_n $= 2\pi f_n$ is the fundamental natural frequency of the soil deposit subjected to vertically propagating shear waves

ψ phase angle

The subscript or superscript zero signifies steady-state amplitude of the respective variable. The bar over a symbol indicates a quantity of a statically equivalent homogeneous deposit.

---

floating piles of various flexural rigidities and lengths, embedded in deep or shallow deposits and subjected to various head restraints. Comprehensive collections of available solutions are given by Poulos & Davis (1980).

In the last few years, a significant amount of research has focused on understanding the fundamental characteristics of the dynamic lateral load–deflexion relationships of piles. The dynamic studies have been primarily motivated by the need to design pile-supported structures against earthquakes and to safely install offshore oil platforms in such areas as the North Sea, the Gulfs of Alaska and Mexico, and the sea off southern California.

The developed dynamic formulations may also be categorized in three broad groups which to some extent correspond to the aforementioned three approaches to the static problem.

(a) The 'dynamic Winkler-foundation' approach which determines the 'spring' characteristics by considering outward propagating waves under horizontal plane-strain conditions (Novak, Nogami & Aboul-Ella, 1978; Novak & Aboul-Ella, 1978; Liou & Penzien, 1977; Kagawa & Kraft, 1980; Dobry, Vicente, O'Rourke & Roesset, 1982).

(b) The analytical elastic continuum-type formulations which enforce the boundary conditions at the soil–pile interface by expanding the contact pressure distribution into a series, in terms of the natural modes of vibration of the deposit (Tajimi, 1969; Nogami & Novak, 1977; Kagawa & Kraft, 1981; Harada, Kubo & Katayama, 1981).

(c) The dynamic finite-element formulations which use axisymmetric elements and special energy-absorbing boundaries to simulate the effect of outward spreading waves (Blaney, Kausel & Roesset, 1976; Kuhlemeyer, 1979; Angelides & Roesset, 1981).

Although considerable progress has been made in developing methods of analysis and understand-

ing the phenomena related to dynamic soil–pile interaction, much has still to be learned through systematic parametric studies, as well as field observations. For instance, the number of published solutions in the form of non-dimensional graphs is very limited, compared to the wealth of available static solutions (Poulos & Davis, 1980). The work presented in this Paper aspires to contribute in reducing this gap between available static and dynamic solutions.

The problem studied in this Paper is that of an end-bearing free-head pile embedded in a non-homogeneous soil stratum of modulus increasing linearly with depth. The study was conducted using an efficient dynamic finite-element formulation, developed by Blaney et al. (1976). An interesting feature of the analysis is that, by allowing the frequency of vibration to approach zero, static solutions are readily recovered which are in excellent agreement with the results of the more conventional static finite-element analyses.

A few studies have appeared on the static lateral behaviour of piles embedded in a linearly non-homogeneous deposit. Poulos (1973) used a simple modification of Mindlin's solution to obtain approximate results, assuming the displacement induced from a point load on two identical points in a non-homogeneous and a homogeneous half-space to be inversely proportional to the respective Young's moduli at these points. As shown subsequently in this Paper, Poulos's results may overpredict the top lateral deflexion of a free-head pile subjected to a horizontal force by nearly 100%, but are more reasonable for other types of loading.

A better, although still approximate, formulation was developed by Banerjee & Davies, 1978, within a boundary element algorithm. In this case, Mindlin's solution was extended to a point load acting at the interface of a two-layer elastic half-space and then empirically extrapolated to a linearly inhomogeneous halfspace. The results of this method are within 25% of the results of finite-element studies. Numerically exact solutions were recently presented by Randolph (1981) who studied the lateral behaviour of flexible piles in linearly non-homogeneous soils and offered algebraic expressions for pile deflexions and moments. He utilized an axisymmetric finite-element formulation incorporating linear-strain triangular elements and resorting to a first-order Fourier expansion in the circumferential direction to inexpensively treat the asymmetric lateral loading.

The static results presented in the Paper complement those available from these previous studies, For flexible piles, our results are in accord with those of Randolph (1981). This work, however, is not limited to flexible piles alone but covers a wide range of the most pertinent problem parameters

for which, to date, only approximate solutions are available (Banerjee & Davies, 1978; Poulos, 1973).

The presented results of the comprehensive dynamic parametric study are new in the geotechnical literature. Particular emphasis is accorded to assessing the effects of soil inhomogeneity on pile deflexions at and above the resonant frequencies of the system. It is shown that the selection of a statically equivalent homogeneous deposit not only depends on the type of loading (force or moment) but also that it does not guarantee an equivalent dynamic performance of the pile. It is also shown that the static criterion of flexibility is inadequate with dynamic loading conditions and a new (dynamic) criterion is proposed, appropriate for a wide range of frequencies.

PROBLEM DEFINITION AND METHOD OF ANALYSIS

The system to be studied is given in Fig. 1. A circular pile of length L and diameter d is embedded in a non-homogeneous soil layer of thickness $H = L$ underlain by a rigid base (bedrock). The pile is assumed to be linearly elastic with constant Young's modulus E_p, and mass density ρ_p. The supporting soil is assumed to be a linear hysteretic material with Young's modulus increasing linearly with depth, in accordance with

$$E(z) = E_s \frac{z}{d} \tag{1}$$

in which E_s is the modulus at a depth of one pile diameter below the surface, and with constant (but arbitrary) Poisson's ratio ν, and mass density ρ_s. The energy dissipating characteristics of the soil when subjected to dynamic deformation are described through a frequency-independent hysteretic damping ratio $\beta(z)$, function of depth. A few
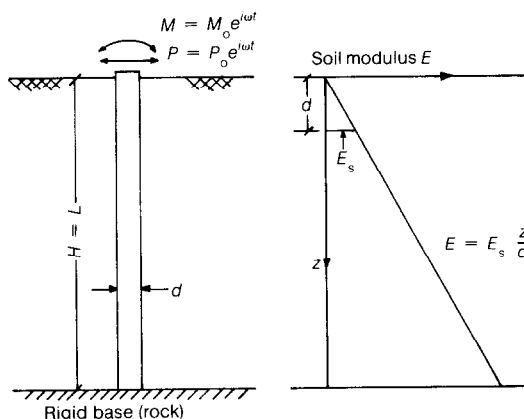

Fig. 1. End-bearing free-head pile under harmonic excitation embedded in a soil stratum with modulus increasing linearly with depth
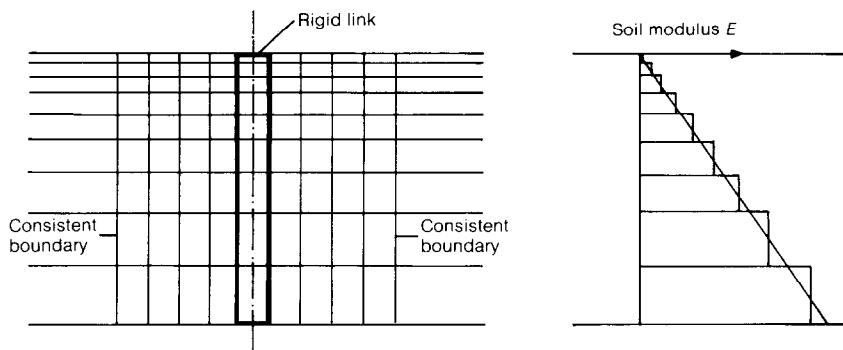
Fig. 2. Finite element model

comments regarding the choice of a linear variation of modulus according to equation (1) are warranted.

Following the work of Gibson (1967, 1974), the elastic halfspace with stiffness proportional to depth (often called Gibson soil) has been frequently used in analytical soil mechanics studies in place of the traditional homogeneous halfspace. The Gibson soil is the simplest possible (one-parameter) inhomogeneous model which appears capable of representing many actual soil profiles with reasonable accuracy. For example, the undrained Young's modulus in normally consolidated clays, being proportional to the effective mean pressure, does increase linearly with depth. Moreover, there is an additional argument in favour of the Gibson soil when modelling the lateral soil reaction against piles. That is, a stiffness proportional to depth may take indirectly into account soil non-linearity, as values of the soil secant modulus near the head of the pile are likely to be reduced because of the developing large shear strains associated with the large pile deflexions near the top.

For the same reason, in response to the increasing soil deformation near the ground surface, hysteretic damping ratio in the soil, $\beta(z)$, should be taken as a decreasing function of depth. In this study, $\beta(z)$ was chosen to vary from a maximum value of 8%, immediately below the surface, to a minimum value of 2% at greater depths; a linear or a parabolic interpolation were assumed for intermediate depths. Sensitivity studies proved that the exact distribution of damping with depths has only a secondary effect on pile response, as long as the average β value remains the same. In fact, it has been shown by the Authors (Krishnan, Gazetas & Velez, 1982) that even use of a constant (i.e. depth-independent) soil damping ratio leads to very good predictions of dynamic pile-head deflexions. Therefore, for simplicity in the presentation, most of the results shown in this Paper were obtained for a constant $\beta(z) = \beta = 5\%$.

The problem studied, as shown in Fig. 1, involves a free-head pile subjected to a steady-state harmonic horizontal force $P = P_0 \exp(i\omega t)$ and/or a moment $M = M_0 \exp(i\omega t)$, with a circular frequency $\omega = 2\pi f$, where f is the frequency in Hz. P_0 and M_0 are the amplitudes of the applied force and moment, respectively. The pile deforms laterally and its steady-state motion at the top may be described in terms of the deflexion

$$u(0) = u_0(0) \exp(i\omega t + \psi_1) \qquad (2a)$$

and the rotation

$$\theta(0) = \theta_0(0) \exp(i\omega t + \psi_2) \qquad (2b)$$

in which ψ_1 and ψ_2 are the phase lags between pile response and excitation, and $u_0(0)$ and $\theta_0(0)$ are the amplitudes of the top deflexion and rotation, respectively. Alternatively, $u(0)$ and $\theta(0)$ may be expressed as

$$u(0) \{u_R(0) + iu_I(0)\} \exp(i\omega t) \qquad (3a)$$

$$\theta(0) = \{\theta_R(0) + i\theta_I(0)\} \exp(i\omega t) \qquad (3b)$$

where $u_R(0)$, $\theta_R(0)$ are the real (in-phase) components and $u_I(0)$, $\theta_I(0)$ are the imaginary (90°-out-of-phase) components of $u(0)$, $\theta(0)$, respectively. Equations (2) and (3) are equivalent; the respective variables are related as

$$u_0(0) = \{[u_R(0)]^2 + [u_I(0)]^2\}^{1/2} \qquad (4a)$$

$$\psi_1 = \arctan[u_I(0)/u_R(0)] \qquad (4b)$$

The finite-element formulation used in this study has been developed by Blaney et al. (1976). The geometry is idealized by a finite cylindrical region surrounding the pile, joined to a semi-infinite far field, as shown in Fig. 2. The cylindrical region is discretized by means of toroidal finite elements and the pile is considered hinged at the base. To overcome the complexity arising from the three-dimensionality of deformation when the pile is subjected to lateral (anti-symmetric) loading, stresses and displacements are expanded into a Fourier series in the circumferential direction,

following the technique devised by Wilson (1965). In fact, only the first order term of the series is needed in this case. Thus, the three-dimensional problem is effectively reduced to a two-dimensional one—a convenient simplification which has also been utilized by Kuhlemeyer (1979) and Randolph (1981).

To account properly for the radiation of energy due to spreading of waves away from the pile, special energy absorbing boundaries have to be devised. The standard boundaries employed in static finite-element formulations are inadequate as they cause an artificial 'box' effect, trapping the wave energy and changing the natural characteristics of the system. In the described programme, a 'consistent' boundary matrix, derived by Kausel (1974), is placed at the outer edge of the central discretized region to reproduce the effect of the far field. This matrix relates the imposed dynamic boundary forces with the resulting displacements of the far field; for each layer, it is obtained from the solution of the appropriate wave propagation problem. A 'perfect' absorption of outward spreading waves is, thus, accomplished. Moreover, the boundary can be placed very close to the pile (only a few diameters away) and hence a substantial economy is achieved. For additional information on the employed formulation reference is made to the aforementioned publications and to Kausel, Roesset & Waas (1975).

PROBLEM PARAMETERS AND DIMENSIONAL ANALYSIS

The generalized force–deformation relations at the (unrestrained) pile head are expressed in non-dimensional form as

$$\frac{u(0)}{d} = U_{HH}\frac{P}{E_s d^2} + U_{HM}\frac{M}{E_s d^3} \qquad (5a)$$

$$\theta(0) = U_{MH}\frac{P}{E_s d^2} + U_{MM}\frac{M}{E_s d^3} \qquad (5b)$$

where U_{HH}, U_{HM}, U_{MH} and U_{MM} are the dimensionless dynamic displacement factors, functions of frequency. By the dynamic reciprocity theorem (Lamb, 1904) $U_{HM} = U_{MH}$. Since $u(0)$ and $\theta(0)$ are complex quantities (equation (3)), the displacement factors can also be written as

$$U_{AB} = R_{AB} + iI_{AB} \quad (AB = HH, HM, MM) \quad (6)$$

where R_{AB} and I_{AB} are the real and imaginary components of U_{AB}. Alternatively, the form

$$U_{AB} = U_{AB}{}^0 \exp(i\omega t + \psi_{AB})$$
$$(AB = HH, HM, MM) \qquad (7)$$

which corresponds to equation (2), is also used in this Paper. $U_{AB}{}^0$ and ψ_{AB} are, respectively, the amplitude and phase-lag of U_{AB}; these are related

to R_{AB} and I_{AB} as indicated by equations (4a) and (4b).

According to the technique of dimensional analysis, the following general functional relation can be stated

$$U_{AB} = F\left(\frac{E_p}{E_s}, \frac{L}{d}, v, \frac{\rho_p}{\rho_s}, a_s, \beta\right) \qquad (8)$$

in which the only independent dimensionless material and geometric parameters of the problem are

(a) the ratio E_p/E_s of the Young's modulus of the pile over the Young's modulus of the soil at a depth of $z = d$
(b) the pile length-to-diameter (slenderness) ratio L/d
(c) the Poisson's ratio of the soil v
(d) the ratio ρ_p/ρ_s of the mass densities of the pile and soil
(e) the dimensionless frequency factor $a_s = \omega d/V_s$, where V_s is the shear wave velocity of the soil at a depth $z = d$, and ω is the excitation circular frequency
(f) the hysteretic damping ratio in the soil, β, assumed to be either a constant or a decreasing function of depth.

In some earlier studies of the dynamic lateral response of piles (Novak & Aboul-Ella, 1978; Nogami & Novak, 1977) the ratio of shear wave velocities V_p/V_s was used to represent the contrast in stiffness between pile and soil. The moduli ratio E_p/E_s was preferred in this study following the suggestions of Blaney et al. (1976) and Dobry et al. (1982), so that the influence of v and ρ_p/ρ_s on the results is minimized. This was also confirmed by our sensitivity studies (see Krishnan et al., 1982). Consequently, although the results to be presented were actually derived for $v = 0.40$ and $\rho_p/\rho_s = 1.60$, they are applicable with good accuracy to soils with $0.30 \leqslant v \leqslant 0.48$* and piles with $1.40 \leqslant \rho_p/\rho_s \leqslant 2.50$. These ranges cover most practical situations.*

A similar observation was made by Randolph (1981), although he suggested the use of $G_s(1 + 3v/4)$ instead of the E_s preferred in this study. Preliminary computations showed that both choices lead to essentially equally small (practically negligible) errors when the $v = 0.40$ results are used for soils with $0.30 \leqslant v \leqslant 0.48$. E_s was, thus,

---

*Although for saturated soft clays under static undrained loading one should use $v = 0.50$, with dynamic loading $v = 0.50$ leads to an infinite dilatational wave velocity which is not observed in the laboratory (Allen, Richarts & Woods, 1980); instead, the Biot–Ishihara theory for poroelastic media yields a maximum value of v somewhat less than 0.50.
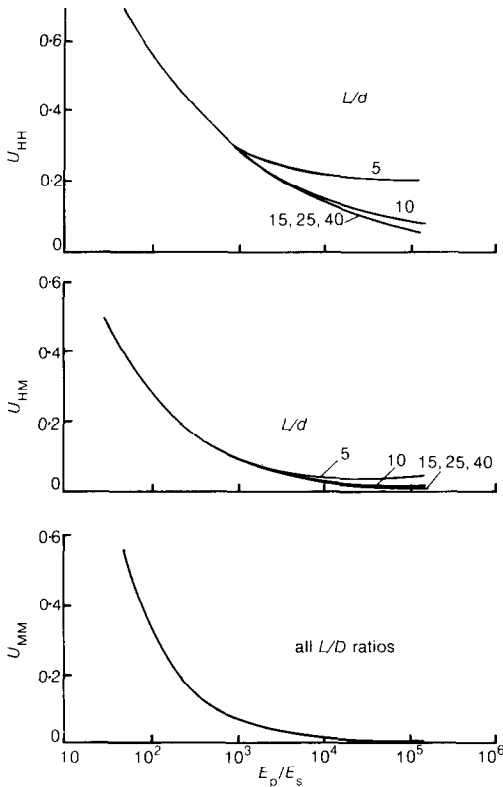
Fig. 3. Dependence of displacement factors on E_p/E_s and L/d

selected in this study as a more convenient parameter.

Frequently, static results are presented in terms of the pile-flexibility factor $K_R = (E_p J_p)/(E_s L^4)$, $J_p = (\pi/64) d^4$, and the slenderness ratio L/d (Poulos & Davis, 1980; Banerjee & Davies, 1978). Although, of course, these parameters are perfectly acceptable from a theoretical viewpoint, they are not very suitable when it comes to the clarity and conciseness in presenting parametric plots. This is because (a) the significance of E_p/E_s is difficult to discern through the K_R factor, as the latter is also affected by $(L/d)^4$; and (b) the importance of L/d is also difficult to readily visualize, since it appears twice. This double appearance of L/d may (erroneously) give the impression that slenderness ratio is the predominant parameter which controls the response. In fact, as it is shown later in this Paper (see also Randolph, 1981), most laterally loaded piles are flexible; only their upper part undergoes substantial deformation and provides lateral resistance. Hence L/d may very well be a totally insignificant parameter. But to find this out, one must read two or three plots of response versus K_R, each for a different L/d value.

The results reported here are based on analyses using five moduli ratios, namely, $E_p/E_s = 58$, 290, 1450, 29 000 and 145 000. For each of these values five slenderness ratios are considered, namely, $L/d = 5$, 10, 15, 25 and 40, and, in every case, the frequency factor a_s is varied from 0·01 to 1·2, encompassing the wide frequency ranges expected from machinery, ocean waves and earthquakes.

STATIC PILE BEHAVIOUR

The present study was conducted for an end-bearing pile, i.e., with length $L = H$ (Fig. 1). However, it is subsequently shown that most of the results are also valid for floating piles, i.e., with length $L < H$.

Figure 3 portrays the dependence of the three static displacement factors, U_{HH}, U_{HM} and U_{MM}, on the two crucial parameters, E_p/E_s and L/d. The three displacement factors are quite insensitive to variations in L/d, except for very short and rigid piles. In fact, U_{MM} is practically independent of L/d, throughout the extreme range of moduli ratio examined; and U_{HM} is slightly influenced by the pile length only if $L/d \leqslant 5$ and $E_p/E_s \geqslant 10 000$. Thus, the lateral response of a free-head pile embedded in a given Gibson stratum and subjected to a static moment at its top is practically independent of the pile length. By contrast, the effect of the pile stiffness is substantial.

The effect of pile length on U_{HH} depends on both the L/d and the E_p/E_s ratios. For $L/d > 15$, U_{HH} is uniquely related to E_p/E_s alone. Decreasing L/d to a value of 10 leads to a slight increase of U_{HH} in case of relatively rigid piles, with $E_p/E_s > 5000$. On the other hand, piles which are extremely short ($L/d = 5$) and rigid ($E_p/E_s > 2000$) exhibit substantially larger U_{HH} values (by a factor of about 2) than their longer ($L/d > 10$) counterparts.

From the preceding observations it is evident that for the majority of piles encountered in practice, pile length plays little or no role in their static deformation. This suggests that the induced deflexions and rotations do not influence the whole length of these piles but, instead, they are confined to their upper region, immediately below the ground surface. Careful examination of the distribution of pile deformations with depth for all the studied cases confirms that, indeed, in most situations, deflexions practically vanish beyond five to ten diameters depth from the ground surface.

Effective length of pile

Adopting the terminology of Kuhlemeyer (1979) and Randolph (1981), effective length, l_s, of a laterally loaded pile is defined as the depth below which pile deflexions are less than one-thousandth of the top deflexion. Piles with length $L > l_s$ are
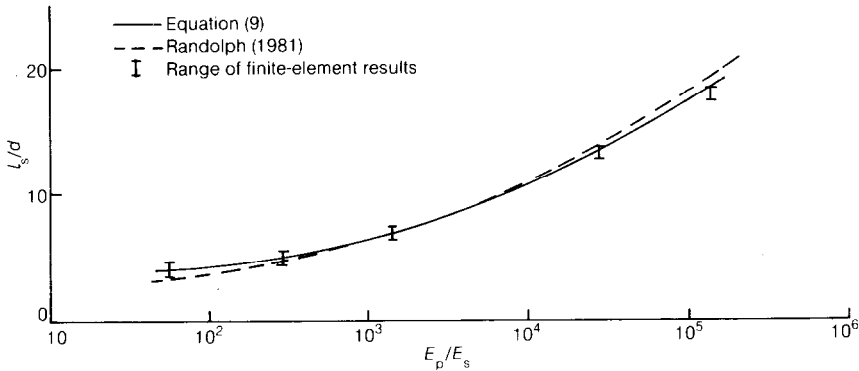
Fig. 4. Variation of the static effective length of pile with E_p/E_s

named flexible* piles. The subscript s is a reminder that the present discussion pertains solely to static loading conditions. Under dynamic loading, the effective pile length, l_d, is generally larger than l_s, as will be shown later.

Figure 4 plots the variation of the effective slenderness ratio l_s/d with E_p/E_s. L/d has no influence on l_s, as long as the pile is flexible. As an example, a pile with $E_p/E_s = 290$ has an $l_s/d \simeq 5$, for all the five lengths studied ($L/d = 5$, 10, 15, 25 and 40); obviously, the shortest of these piles ($L/d = 5$) is a borderline case ($l_s = L$). On the other hand, in the range of very rigid piles ($E_p/E_s > 10\,000$), $l_s/d > 10$, and hence only the three longest piles ($L/d = 15$, 25 and 40) are flexible.

It is now clear why most of the presented results are applicable to floating as well as end-bearing piles. Removing the 'idle' portion of a pile below the depth $z = l_s$ will have no measurable effect on its lateral response.

The following simple algebraic expression fits the data points of Fig. 4 with very good accuracy

$$\frac{l_s}{d} \simeq 1\cdot45\left(\frac{E_p}{E_s}\right)^{0\cdot21} \qquad (9)$$

This expression is only insignificantly different from the formula given by Randolph (1981); for comparison, the latter is also plotted in Fig. 4 for $v = 0\cdot40$. It is emphasized that the effective length of equation (9) corresponds to U_{HH}, i.e., to deflexions due to a sole horizontal force. U_{HM} and, especially, U_{MM} decay much faster with depth, as is indirectly evident from the plots of Fig. 3. In other words, l_s of equation (9) is actually the largest (and, thus, the critical) effective length, for the static loading conditions examined herein.

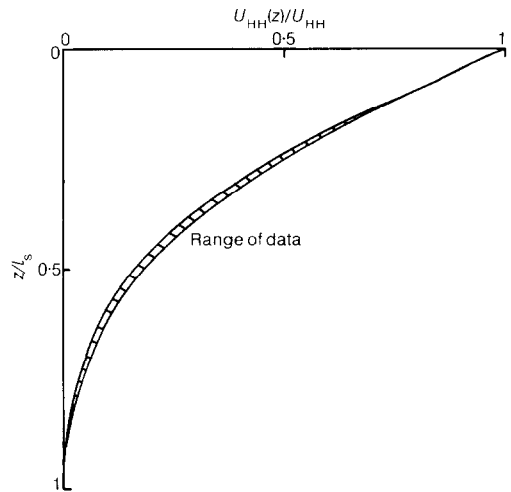* The term long piles is also found in the literature (e.g., Dobry et al., 1982).

Fig. 5. Profile of normalized horizontal pile displacement due to a horizontal force

Behaviour of flexible piles

An interesting observation can be made regarding the deflected shape of flexible piles subjected to a horizontal force. To this end, Fig. 5 portrays the distribution of $U_{HH}(z)$, normalized to a unit top amplitude, against the normalized depth z/l_s. The results for all the 19 flexible piles of this study fall within a very narrow band. This suggests that the deflected shape is a unique function of z/l_s, being otherwise independent of both E_p/E_s and L/d, in agreement with Randolph (1981). The simple algebraic expression

$$U_{HH}(z)/U_{HH} = \left(1 - 0\cdot95\frac{z}{l_s}\right)^{5/2} \qquad (10)$$

fits well the data of Fig. 5 [$U_{HH} \equiv U_{HH}(0)$ denotes the value of the displacement factor at the pile-head (equation (3a))].

Since the response of flexible piles is independent of their length, simple, readily applicable

Table 1. Expressions for displacement factors of flexible piles embedded in non-homogeneous soil

Type of pile	Displacement factor	Expression
Free-head	U_{HH}	$2 \cdot 50 \, (E_p/E_s)^{-0 \cdot 31}$
	U_{MM}	$8 \cdot 80 \, (E_p/E_s)^{-0 \cdot 73}$
	U_{HM}	$2 \cdot 75 \, (E_p/E_s)^{-0 \cdot 50}$
Fixed-head	$U_{HH}{}^{*}\dagger$	$1 \cdot 70 \, (E_p/E_s)^{-0 \cdot 36}$

$\dagger \; U_{HH}{}^{*} = E_s \, du^{*}(0)/P$; $u^{*}(0) =$ horizontal pile-head displacement with $\theta^{*}(0) = 0$
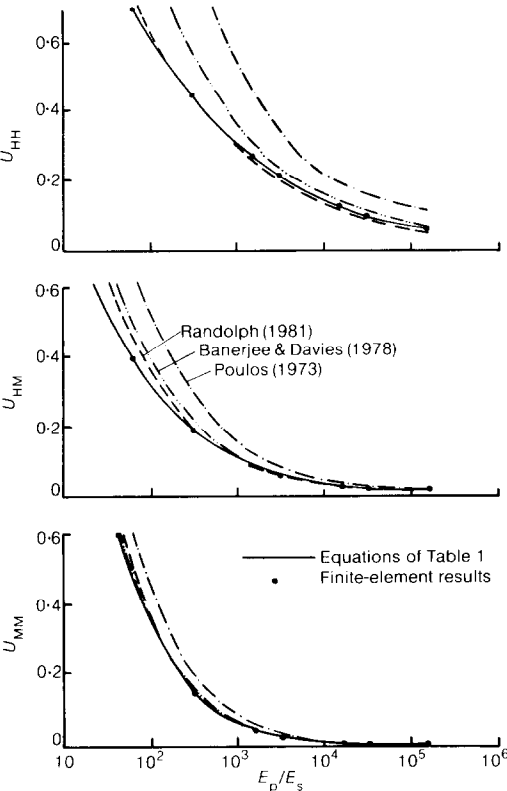
Fig. 6. Comparison of finite-element results for flexible piles with the formulae of Table 1 and the results of some previous solutions

algebraic formulae have been derived for the displacement factors from the pertinent results of Fig. 3. Table 1 displays these expressions which relate U_{HH}, U_{MM} and U_{HM} to the stiffness ratio, E_p/E_s. For completeness, the horizontal displacement factor $U_{HH}{}^{*}$ for a fixed-head pile is also presented; $U_{HH}{}^{*}$ is proportional to the horizontal displacement over horizontal force ratio, when no rotation is allowed at the top. These expressions, as well as the plots of Fig. 3, reveal that pile response to moment loading exhibits a substantially stronger dependence on E_p/E_s than pile response to a horizontal force.

Figure 6 shows that the proposed expressions and the finite-element results match very well, for all practical applications. Randolph's (1981) expressions for $v = 0 \cdot 40$, also plotted in this figure, compare favourably with the formulae of Table 1, although he predicts a slightly stronger dependence of the three free-head displacement factors on E_p/E_s (exponents respectively equal to $-0 \cdot 33$, $-0 \cdot 55$ and $-0 \cdot 78$ in place of the $-0 \cdot 31$, $-0 \cdot 50$ and $-0 \cdot 73$ of this work). On the other hand, the approximate formulations by Banerjee & Davies (1978) and by Poulos (1973) overestimate the three displacement factors; the discrepancies are substantial for horizontal-force loaded piles of $E_p/E_s < 1000$, but reduce significantly as E_p/E_s increases. Moment loading conditions, however, seem to be reasonably well reproduced in these two formulations, especially the more rigorous one of Banerjee & Davies (1978).

Statically equivalent homogeneous deposits

Frequently, practising geotechnical engineers involved in the design of piles and foundations to be embedded in non-homogeneous soil make use of published solutions developed for homogeneous soils (such as those presented by Poulos & Davis, 1980, and Gazetas, 1983). To this end, they must select an appropriate equivalent modulus, corresponding to a representative or effective point in the actual (non-homogeneous) profile. Equivalence between homogeneous and actual profiles is established with respect to a particular response quantity.

For laterally loaded piles embedded in a linearly inhomogeneous soil deposit the depth from ground surface of the representative point (hereafter called equivalent depth) depends not only on the pile geometry and stiffness but also on the type of loading (Fig. 7). Indeed, the equivalent depth $\bar{z}_{HH}$ which leads to the same horizontal deflexion under the sole action of the same horizontal force, differs from the equivalent depths $\bar{z}_{MM}$ and $\bar{z}_{HM}$ which establish equality of top rotation and top deflexion, respectively, under the sole action of a moment.

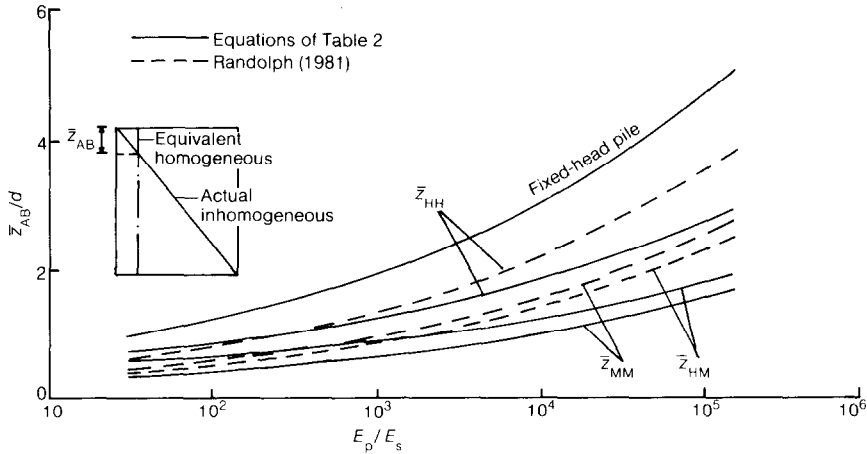Table 2 displays simple formulae for the equiva-

Fig. 7. Variation of equivalent depths with E_p/E_s for flexible piles

Table 2. Formulae of statically equivalent depths for flexible piles

Type of pile	Equivalent depth	Expression
Free-head	$\bar{z}_{HH}$	$0.38d\,(E_p/E_s)^{0.17}$
	$\bar{z}_{MM}$	$0.16d\,(E_p/E_s)^{0.20}$
	$\bar{z}_{HM}$	$0.34d\,(E_p/E_s)^{0.14}$
Fixed-head	$\bar{z}_{HH}{}^*$	$0.48d\,(E_p/E_s)^{0.20}$

lent depths $\bar{z}_{HH}$, $\bar{z}_{MM}$, $\bar{z}_{HM}$ and $\bar{z}_{HH}{}^*$ of flexible piles. $\bar{z}_{HH}{}^*$ refers to the deflexion of a fixed-head pile. These formulae were derived by equating the appropriate asymptotic expressions for flexible piles in a linearly non-homogeneous (Table 1) and in a homogeneous deposit (Kuhlemeyer, 1979; Dobry *et al.*, 1982). Use of Randolph's (1981) expressions for $v = 0.40$ leads to only slightly different expressions.

The expressions of Table 2 are graphically illustrated in Fig. 7. The effective point for the majority of flexible piles in a linearly non-homogeneous soil lies only about one to two diameters beneath the surface, depending on the loading conditions. Moment loading leads to the shallower equivalent depths and fixed-head loading to the deepest.

Physical explanation of these features observed in Fig. 7 is straightforward: the faster the induced pile deformations decay with depth, the shallower the effective point is located. In a non-homogeneous stratum, the near-surface soil modulus is very small and, hence, flexible piles experience large top deflexions which attenuate within a few diameters depth. For instance, Fig. 5 suggests that $U_{HH}(z)$ reduces to $\frac{1}{2}$ of its surface value at a depth of

$l_s/4$; since for most piles $l_s \simeq 4d$ to $8d$ (Fig. 4), the major pile deflexions seem to be confined within a depth of one or two diameters. Naturally, the effective point would also be located in this region.

Moment loading causes deflexions of a free-head pile (proportional to $U_{MH}(z)$) which exhibit an even greater concentration near the top (see Fig. 8); thus, $\bar{z}_{HM} < \bar{z}_{HH}$. On the other hand, horizontal displacements of a fixed-head pile remain substantial for relatively large depths—a direct consequence of the imposed no head-rotation constraint; therefore, $\bar{z}_{HH}{}^* > \bar{z}_{HH}$. Furthermore, regardless of loading conditions, increasing the relative flexural rigidity of a pile would increase the deformations experienced at larger depths and decrease their concentration near the surface; hence, equivalent depths invariably increase significantly with E_p/E_s.

DYNAMIC PILE BEHAVIOUR
General characteristics of the dynamic response

Figure 9 portrays the variation of the three (dynamic) displacement factors with frequency of excitation, for a pile with $L/d = 15$, $E_p/E_s = 29\,000$ and $\rho_p/\rho_s = 1.6$. Both the real (in-phase) and the imaginary ($90°$-out-of-phase) components of each displacement factor (see equation (6)) are displayed; for completeness, the amplitudes and phase angles of the three factors (equation (7)) are also plotted in Fig. 9b. The real displacement components reflect the stiffness and inertia of the soil–pile system; their dependence on frequency is attributed solely to the influence which frequency exerts on inertia, since soil properties are practically frequency-independent. The imaginary components, on the other hand, reflect the radiation and material damping of the system.
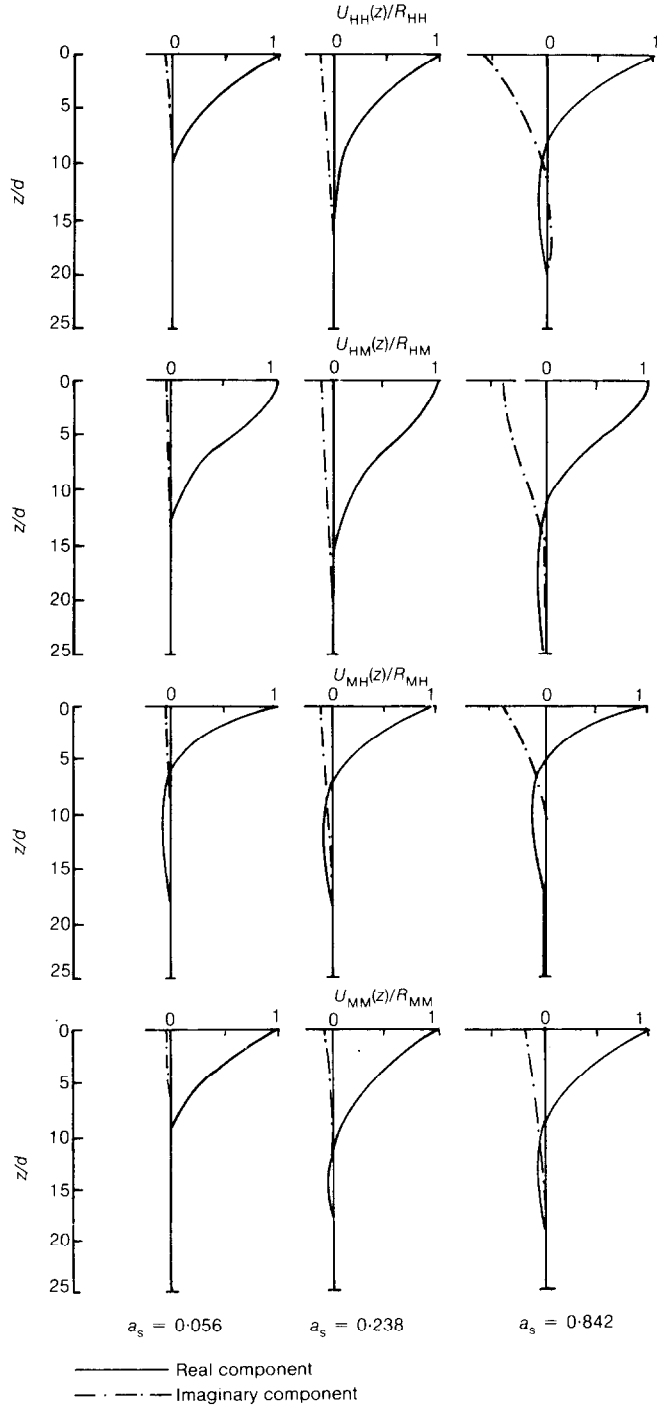
Fig. 8. Distribution of dynamic deformations with depth at frequency
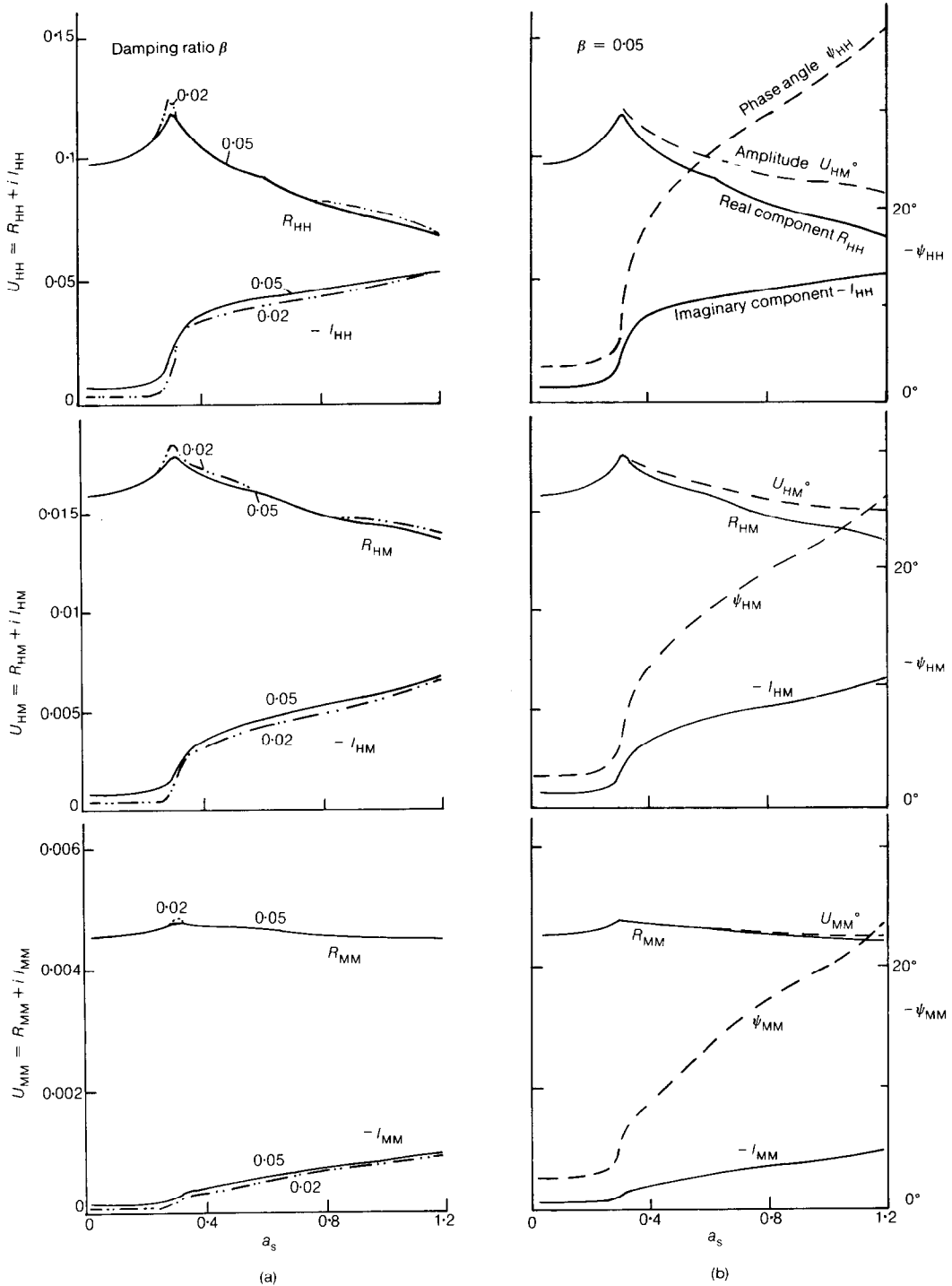factors $a_s = 0.056$, 0.238 and 0.842 ($E_p/E_s = 29\,000$, $L/d = 25$)

Fig. 9. **Dynamic head-deflexions and rotations of a pile with $E_p/E_s = 29\,000$ and $L/d = 15$: (a) effect of damping ratio (0·02 vs 0·05); (b) comparison of the two alternative representations of deformations, equations (6) and (7), for a 0·05 damping ratio**

Material damping stems mainly from the hysteretic cyclic behaviour of soil and is practically frequency-independent, while radiation damping depends strongly on frequency since it results from the spreading of energy by waves generated at the pile–soil interface.

Two sets of results are shown in Fig. 9a, corresponding to low (0·02) and moderate (0·05) material damping in the soil. Several major features of the dynamic response are worthy of note in this figure.

In general, the imaginary components I_{AB} of the displacement factors or the phase angles ψ_{AB} show a greater sensitivity to variations in the frequency factor a_s than the real components or the amplitudes do. A possible exception is the sharp peak of R_{HH} in soils with very small hysteretic damping.

While all three imaginary components are monotonically increasing functions of a_s, the real components exhibit undulations associated with the natural frequencies (in shear and dilatation) of the soil stratum. In other words the observed peaks are the outcome of resonance phenomena. Waves emanating from the oscillating pile–soil interface undergo multiple reflections at the bedrock and the ground surface, creating standing waves; resonance occurs when at a specific frequency the displacement pattern of these standing waves coincides with a natural mode of vibration of the soil stratum. As a result, the amplitude of pile motion may substantially increase, depending on the amount of hysteretic damping in the soil.

The first resonant frequencies of R_{HH} and R_{HM} are in remarkably close agreement with the fundamental natural frequency of the soil stratum in vertically propagating shear waves. Indeed, for a Gibson stratum of thickness $H = L$ and modulus given by equation (1), Dobry, Whitman & Roesset (1971) give the following expression for the natural circular frequencies in shear

$$\omega_n = \frac{x_n}{2}\frac{V_s}{H}\left(\frac{L}{d}\right)^{\frac{1}{2}} \quad n = 1, 2, 3, \dots \quad (11)$$

where x_n is the nth root of $J_0(x) = 0$, in which J_0 is the Bessel function of the first kind and zero order. (For example, $x_1 \simeq 2\cdot40$, $x_2 \simeq 5\cdot52$, etc.) Hence the fundamental natural frequency factor $a_{s,1}$ becomes

$$a_{s,1} = \frac{\omega_1 d}{V_s} \simeq 1\cdot20\left(\frac{L}{d}\right)^{-0\cdot50} \quad (12)$$

For $L/d = 15$ equation (12) gives $a_{s,1} \simeq 0\cdot31$ which almost coincides with first resonant frequency factor of R_{HH} and R_{HM} observed in Fig. 9. This coincidence suggests that essentially only shear waves propagate in the stratum at this frequency (unambiguous or total resonance).

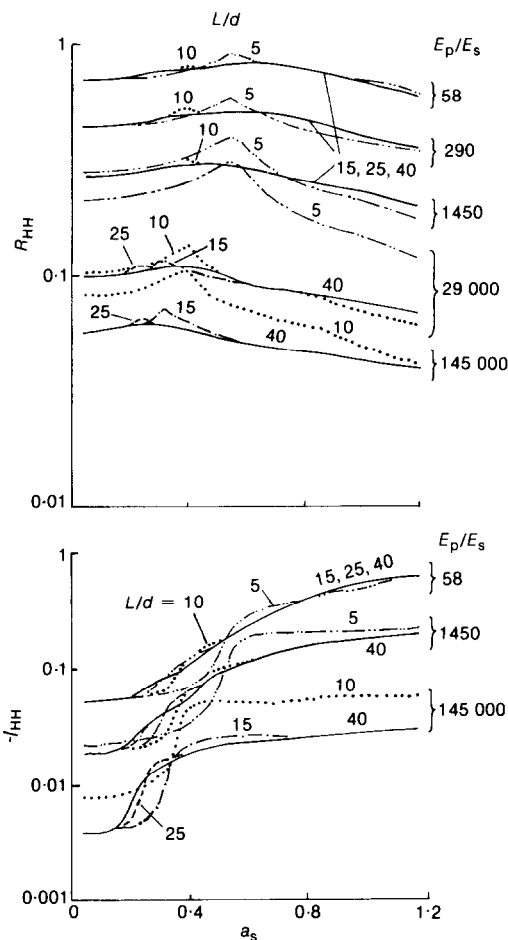The second peaks of R_{HH} and R_{HM}, on the other

Fig. 10. Dynamic displacement factor $U_{HH} = R_{HH} + iI_{HH}$ as a function of a_s, E_p/E_s and L/d ($\beta = 0\cdot05$)

hand, are barely noticeable, occurring at a frequency factor of about 0·66. Instead, equation (11) yields for the second natural frequency of the deposit in shear waves: $a_{s,2} \simeq 0\cdot71$. Hence, clearly, more than one type of wave is present in the stratum at these frequencies (pseudo or partial resonance).

Another important phenomenon is revealed through the variation of the imaginary displacement factors with a_s. At low frequencies, below the first resonant frequency, radiation damping is zero. This is because no surface waves can be physically created in a soil stratum at such frequencies and, since the bedrock prevents waves from propagating downward, geometrical spreading of wave energy is negligible. The small values of the imaginary components I_{AB} or the phase angles ψ_{AB} in this range (Fig. 9) just reflect the energy loss through hysteretic damping; for a purely elastic
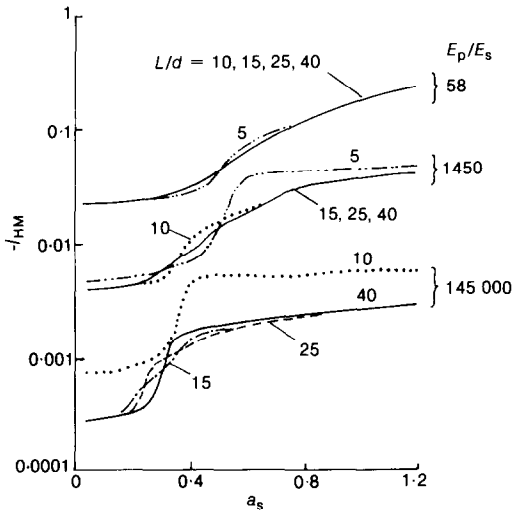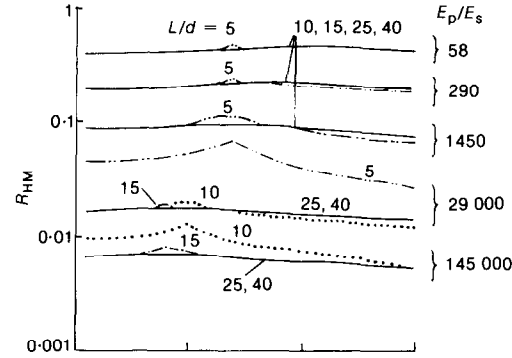
Fig. 11. Dynamic displacement factor $U_{HM} = R_{HM} + iI_{HM}$ **as a function of** a_s, E_p/E_s **and** L/d ($\beta = 0.05$)
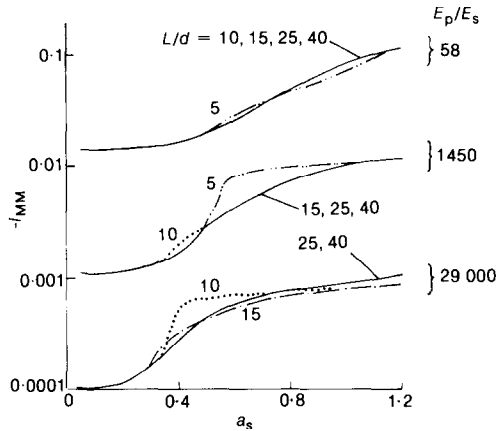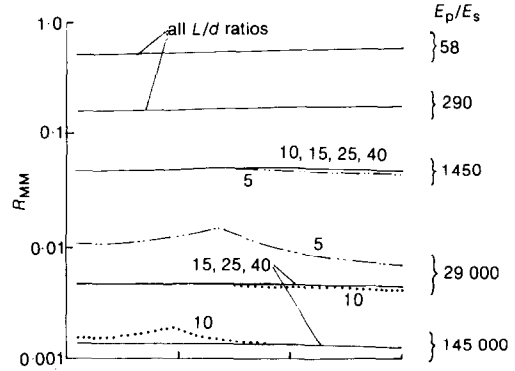

Fig. 12. Dynamic displacement factor $U_{MM} = R_{MM} + iI_{MM}$ **as a function of** a_s, E_p/E_s **and** L/d ($\beta = 0.05$)

soil I_{AB} and ψ_{AB} would be zero in this (low) frequency range.

This lack of radiation damping at $a_s \leqslant a_{s,1}$ explains the sharpness of the peak at first resonance. On the contrary, radiation damping, being ever present at higher frequencies, is primarily responsible for suppressing the second (pseudo-resonant) peak.

Two main differences are observed between pile response in rocking (U_{MM}) and in swaying (U_{HH}). First, the real component of rotation R_{MM} is very insensitive to variations in a_s and its resonant peaks are hardly noticeable; therefore, assuming R_{MM} to be frequency-independent would be a most reasonable simplification. Second, even at frequencies beyond $a_{s,1}$, the imaginary component of rotation I_{MM} and the phase angle ψ_{MM} attain disproportionately small values, in comparison with the values of I_{HH} and ψ_{HH}. This suggests that

only a small amount of radiation damping arises during rocking oscillations—a phenomenon reminiscent of the rocking of shallow foundations (Gazetas, 1981, 1983). Indeed, constructive interference of the shear and dilatational waves emanating from the pile–soil interface during rocking does not favour the generation of surface waves which are the main carriers of radiation damping.

Finally, the similarity between the in-phase (real) component and the amplitude of a displacement factor, as well as between its 90°-out-of-phase (imaginary) component and its phase angle, are evident from Fig. 9b. In the low frequency range, in particular, due to negligible radiation damping, the amplitudes of motion practically coincide with its in-phase components, while the phase angles reflect the hysteretic damping in the soil. At higher frequencies, due to increasing importance of radiation damping, the amplitudes of motion exceed the
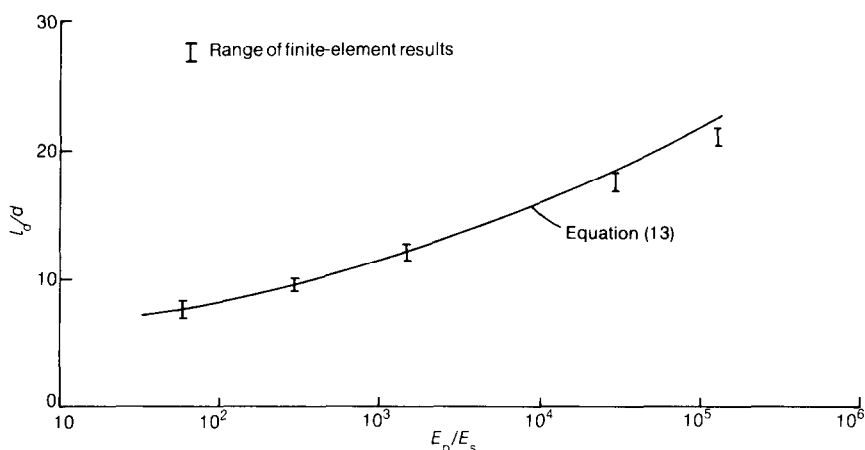
Fig. 13. Variation of dynamic effective length with E_p/E_s

respective real components but the phase angles increase with a_s more rapidly than the imaginary components do. Overall, however, the two alternative presentations of the dynamic displacement factors, i.e. (R_{AB}, I_{AB}) and $(U_{AB}{}^0, \psi_{AB})$, convey the same information and reveal in a similar way the various trends in the response; thus, only the (R_{AB}, I_{AB}) decomposition (equation (6)) is used in the sequel.

Parameter study: stiffness and slenderness ratios

The influence of E_p/E_s and L/d on the dynamic pile-head deflexions and rotations is graphically illustrated in Figs 10, 11 and 12 for a range of a_s values between almost 0 and 1·2. The practical usefulness of these plots stems from their non-dimensional form and the wide range of pertinent parameters considered. Several trends are worthy of note.

(a) Pile response at a given frequency is mainly a function of E_p/E_s, being relatively insensitive to variations in L/d. Very short and rigid piles are the exception (e.g., $L/d \leqslant 5$, $E_p/E_s > 20\,000$). Their response is nearly independent of E_p/E_s and strongly dependent on L/d. For the sake of clarity of the graph the $L/d = 5$ and $E_p/E_s = 145\,000$ response curve is not plotted in these figures, as it nearly coincides with the $L/d = 5$ and $E_p/E_s = 29\,000$ curve.

(b) The primary role of L/d is to control the frequency and amplitude of first resonance. Decreasing L/d increases both the resonant frequency, according to equation (12), and the resonant amplitude of all three displacement factors. On the other hand, at high frequency factors (in excess of $a_{s,1}$), decreasing L/d increases the radiation damping of the system; hence real components (and amplitudes) tend to decrease while imaginary components (and

phase angles) increase. The magnitude of these effects depends to a large extent on E_p/E_s: the changes are insignificant for very soft piles ($E_p/E_s = 58$) but substantial for very stiff piles ($E_p/E_s = 145\,000$).

(c) The second (pseudo) resonances are hardly noticeable with the logarithmic scales chosen for the ordinates of Figs 10–12, except in the case of very stiff and short piles.

(d) For the range of parameters appropriate for the majority of piles in practice, R_{MM} and R_{HM} are essentially frequency-independent and one needs only to predict correctly their static values (e.g. Fig. 3).

(e) Finally, it is evident that many piles which exhibit a flexible (length-independent) static behaviour cannot be considered flexible under dynamic loads, at frequencies near resonance. An example: a pile of $L/d = 15$ and $E_p/E_s = 29\,000$ is statically flexible ($L > l_s \simeq 13d$ from Fig. 4); at resonance, however, its R_{HH} is about 15% higher than the corresponding value of a pile with $L/d = 40$ and the same stiffness ratio. Although this is a rather modest difference, it is worth exploring the causes of such an effect.

Flexible behaviour under dynamic loads

Figure 8 portrays a typical set of distributions of dynamic deformations with depth, experienced by a pile of $E_p/E_s = 29\,000$ and $L/d = 25$ at three different frequencies of excitation ($a_s = 0.056, 0.238$ and 0.842). Under static loading this pile deforms appreciably only at its uppermost $13d$, according to Fig. 4—a clearly flexible behaviour which does not change to any measurable degree during oscillation at low frequency factors, as evidenced by the deformation distributions at $a_s = 0.056$ (Fig. 8).
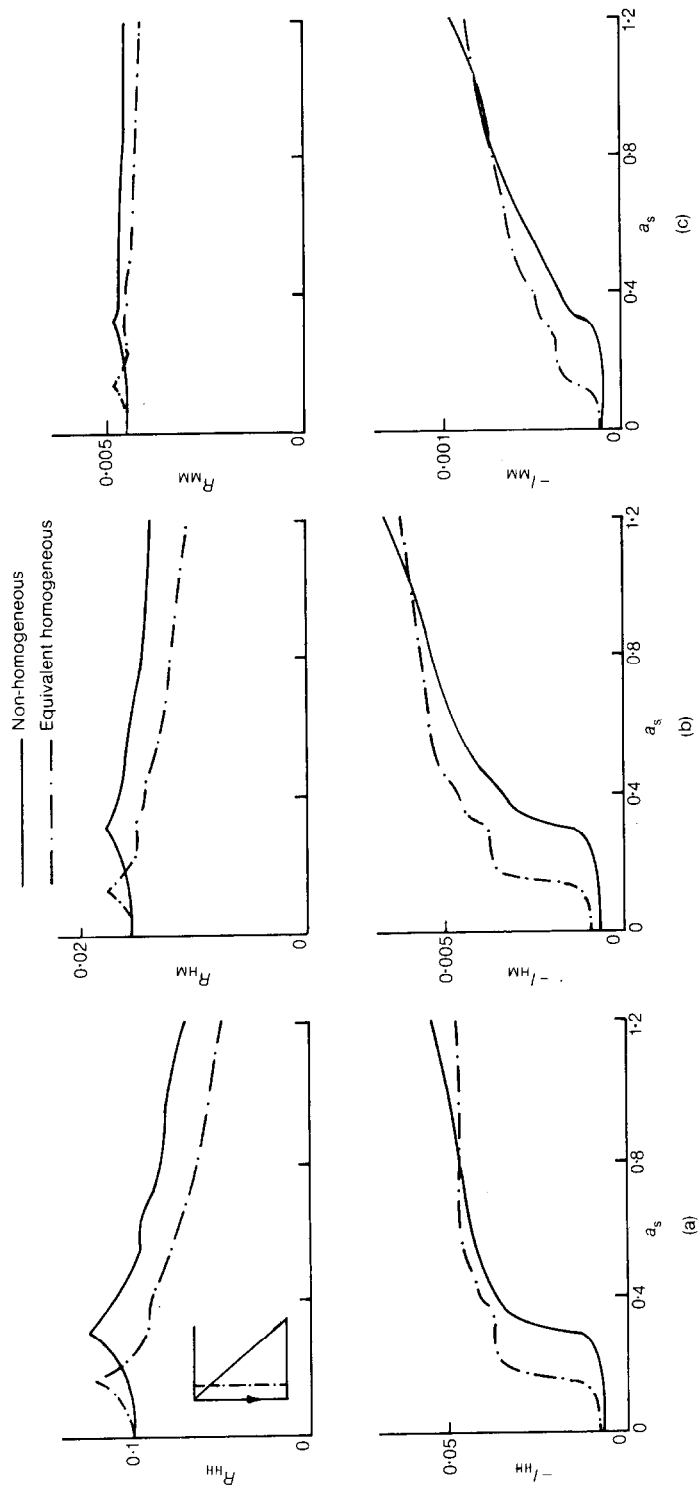
As the excitation frequency increases, however,

Fig. 14. Comparison of the dynamic response of a pile with $E_p/E_s = 29\,000$ and $L/d = 15$ embedded in the non-homogeneous and statically equivalent homogeneous deposits for three modes of deformation: (a) HH; (b) HM; (c) MM
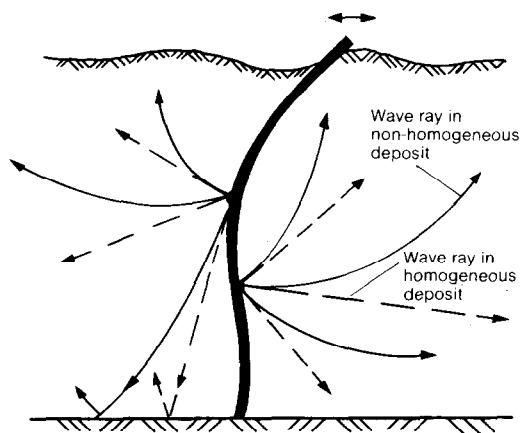
Fig. 15. Upward reflection of waves generated in the non-homogeneous stratum may increase the motion at the pile head

pile deformations extend to greater depths. In particular, at the fundamental frequency of the system ($a_s \simeq 0.238$ according to equation (12) or Fig. 10) deflexions are sustained by a pile length of about $17d$. The deformed shape of the pile, on the other hand, undergoes only minor changes in the frequency range $0 \leqslant a_s \leqslant a_{s,1}$. Thus, if, for instance, $U_{HH}^0(z)/U_{HH}^0$ or $R_{HH}(z)/R_{HH}$ at a particular frequency is plotted against the normalized depth z/l_d, where l_d = the effective length at that frequency, the static variation of equation (10) or Fig. 5 is recovered with reasonable accuracy. And since, in this frequency range, l_d is maximum at the fundamental frequency of the system, this length, at $\omega = \omega_1$, is defined as the (critical) effective dynamic length, l_d, of the pile. The dependence of l_d on d and E_p/S_s is displayed graphically in Fig. 13 with the simple expression

$$\frac{l_d}{d} \simeq 4.47 \left(\frac{E_p}{E_s}\right)^{0.135} \qquad (13)$$

being offered for direct practical use.

The deformation patterns at higher frequencies also reveal some interesting response characteristics. Beyond the fundamental frequency ω_1 the shape of the deforming pile can no longer be described through equation (10) or Fig. 5. Instead, the variations with depth of both real and imaginary deformation components display a wavy character, with the upper and lower parts of the pile moving in opposite directions. At the same time the contribution of the imaginary components substantially increases. But although pile deformations at very high frequencies may extend all the way to the bottom of the pile, top deflexions and rotations indicate a flexible, i.e. length-independent, behaviour (Figs 10–12).

In conclusion, pile response at resonance is critical for judging its dynamic flexibility, defined as length-independency of top motion. Piles with $L > l_d$ as given by equation (13) will behave as flexible in all but a few frequencies at and near resonance; but even at these frequencies, their response will be within merely 6% above the response of the clearly flexible (very long) piles. This is a minor difference in view of the uncertainties in determining soil properties and loads. Thereby, equation (13) can be recommended for practical use (especially in preliminary design computations) in deciding on the nature of the dynamic pile behaviour. It is emphasized, however, that top deformations (alone) form the basis of the flexibility criterion. Requiring length-independency of another response quantity, such as the maximum bending moment in the pile, would undoubtedly impose a different (more stringent) effective length criterion.

Importance of soil non-homogeneity

A convenient way to study the effects of non-homogeneity on the dynamic lateral response of piles is to compare them with the results for a statically equivalent homogeneous stratum. Such a comparison is shown in Fig. 14 for a free-head pile with $L/d = 15$ and $E_p/E_s = 29\,000$. The response of such a pile embedded in a linearly inhomogeneous stratum has already been described (Figs 9–12). For each of the three modes of deformation, HH, HM and MM, a statically equivalent homogeneous deposit, yielding identical static response, can be readily determined using the formulae presented in Table 2, in conjunction with equation (1). The respective dynamic response of the pile in each of the three equivalent deposits (obtained using the aforementioned finite-element formulation) is compared in Fig. 14 with its response in the non-homogeneous stratum.

It is evident from this figure that static equivalence does not guarantee identical behaviour under dynamic loads. The two main differences between homogeneous and inhomogeneous behaviour may be summarized and explained as follows.

The first difference is that their resonant frequencies differ by a factor of about 2. To understand the cause of such a potentially serious discrepancy recall that the representative or effective point which controls the static response in the non-homogeneous deposit lies only one or two diameters below the surface (Table 2, Fig. 7). Thus, the statically equivalent homogeneous deposit has an S-wave velocity quite smaller than the velocity at mid-depth of the inhomogeneous stratum (see insert in Fig. 14a). However, the representative point which controls the fundamental frequency of

the stratum is located slightly below its mid-depth; hence, for vertical shear wave propagation the homogeneous deposit is much softer and leads to a smaller resonant frequency. As an example: for a pile of $E_p/E_s = 29\,000$ and $L/d = 15$ the equivalent depth for the HH mode is $\bar{z}_{HH} \simeq 2.17d$ (Table 2) leading to a fundamental natural frequency for the homogeneous deposit (see e.g., Dobry *et al.*, 1971)

$$\bar{\omega}_1 = \frac{\pi}{2} \frac{V_s}{L} \left(\frac{\bar{z}_{HH}}{d} \right)^{1/2} \simeq 2.31 \frac{V_s}{L} \qquad (14)$$

and a resonant frequency factor $\bar{a}_{s,1} = 2.31$ $(d/L) \simeq 0.154$—in agreement with Fig. 14a. On the other hand, equation (12) yields for the resonant frequency of the inhomogeneous deposit $a_{s,1} \simeq 0.31$, which is twice $\bar{a}_{s,1}$.

The second difference in behaviour between homogeneous and inhomogeneous strata is that they have different responses at high frequencies. The inhomogeneous profile leads invariably to the larger in-phase and the faster growing (with a_s) $90°$-out-of-phase components of head-deformation. The complicated system of dilatational, shear and surface waves that are present at such frequencies precludes a clear-cut explanation of the observed differences. It seems, nonetheless, that one of the possible causes of stronger inhomogeneous motion is the continuous upward reflection of waves originating at the pile–soil interface. The phenomenon is reminiscent of the total reflection of waves emanating from a surface foundation into an inhomogeneous halfspace (Gazetas, 1980). As shown in Fig. 15, a wave ray in a non-homogeneous medium is not a straight line but a curve. Therefore, waves emanating from a point on the pile surface (Huygen's principle) in an upward direction may very well be deflected towards the pile head; this is impossible in a homogeneous medium.

CONCLUSION

A systematic parametric study has been presented of the static and dynamic deformation of laterally loaded free-head piles embedded in a soil deposit, the modulus of which increases linearly with depth. It has been shown that the ratio of pile Young's modulus to soil modulus at a one-diameter depth is the most significant parameter which controls the response. The slenderness ratio is of secondary importance, except in cases of stiff piles embedded in soft soils. Non-dimensional graphs are presented from which one can readily estimate both static and dynamic deflexions of piles in practice.

Quite frequently piles exhibit a flexible (i.e. length-independent) behaviour under static loading. In most cases, the effective pile length that is needed to transfer static lateral loads into the

ground and below which insignificant pile deformations occur, extends only 5 to 10 diameters from the surface. However, under dynamic loading the effective pile length increases by an amount that depends mainly on the frequency of excitation.

The concept of a representative point in the soil deposit has been introduced to obtain the properties of a statically equivalent homogeneous deposit. It has been demonstrated that the depth of such a point below the surface depends on the type of pile loading considered. Furthermore, substantial differences are observed in the dynamic response of a pile embedded in the actual non-homogeneous and the equivalent homogeneous stratum. Valuable insight to the mechanics of the problem has been gained by trying to explain these discrepancies at resonance and at high frequency factors.

APPENDIX 1. ILLUSTRATIVE EXAMPLE

The dynamic response of a laterally loaded free-head pile embedded in a clay stratum is estimated below using the graphs and formulae presented in the Paper.

Pile geometry and properties:
(–) circular concrete pile
(–) diameter $d = 0.35$ m
(–) length $L = 20$ m
(–) Young's modulus $E_p = 2.5 \times 10^7$ kPa
(–) mass density $\rho_p = 2510$ kg/m^3

Soil profile
(–) stratum of normally consolidated saturated clay
(–) undrained Young's modulus divided by effective overburden pressure $E/\sigma_v' = 250$
(–) mass density $\rho_s = 1680$ kg/m^3
(–) Poisson's ratio $v = 0.49$
(–) estimated hysteretic damping ratio $\beta = 0.05$

Excitation
A horizontal force $P = 100 \exp(i\omega t)$ kN and a moment $M = 100 \exp(i\omega t)$ kN m are acting simultaneously (in phase) on the pile head at ground–surface level. The frequency of excitation $\omega = 8\pi$ rad/s.

Computations
(–) unit weight of clay $\gamma_s = \dfrac{1680 \times 9.81}{1000} \simeq 16.5$ kN/m^3

(–) Young's modulus of clay
$$E = 250 \gamma_s' z = (250)(16.5 - 10)z = 1625z$$

(–) Young's modulus at $z = d$:
$$E_s = 1625 \times 0.35 \simeq 569 \text{ kPa}$$

(–) stiffness ratio $E_p/E_s = 2.5 \times 10^7/569 \simeq 43937$
(–) slenderness ratio $L/d = 20/0.35 \simeq 57.1$
(–) mass density ratio $\rho_p/\rho_s = 2510/1680 \simeq 1.5$
(–) S-wave velocity at depth $z = d$

$$V_s = \left\{ \frac{E_s/\rho_s}{2(1 + v_s)} \right\}^{1/2} \simeq \left\{ \frac{569/1.68}{2 \times 1.49} \right\}^{1/2} \simeq 10.7 \text{ m/s}$$

(–) frequency factor $a_s = 8\pi(0.35)/10.7 \simeq 0.82$

(-) effective pile length (equation (13)): $l_d \simeq 4 \cdot 47 \ (0 \cdot 35)$ $(43937)^{0 \cdot 135} \simeq 6 \cdot 6 \ \mathrm{m}$, which is substantially smaller than the total pile length, $L = 20 \ \mathrm{m}$; i.e. the pile is flexible, and the exact value of L/d is of little interest.

The normalized displacement factors, F_{HH}, F_{HM} and F_{MM}, may now be estimated from the pertinent plots of an $L/d = 40$ pile shown in Figs 10–12. By linearly interpolating between the '$E_p/E_s = 29\,000$' and '$E_p/E_s = 145\,000$' curves one obtains

$$F_{HH} \simeq 0 \cdot 084 + i(-0 \cdot 05)$$

$$F_{HM} = F_{MH} \simeq 0 \cdot 014 + i(-0 \cdot 0045)$$

$$F_{MM} \simeq 0 \cdot 003 + i(-0 \cdot 0005)$$

The deflexion and rotation at the pile-head can now be computed using equation (5)

$$\begin{aligned} u(0) &= \frac{P}{E_s d} F_{HH} + \frac{M}{E_s d^2} F_{MH} \\ &= \frac{100}{569 \times 0 \cdot 35} (0 \cdot 084 - i0 \cdot 05) \\ &\quad + \frac{100}{569 \times 0 \cdot 35^2} (0 \cdot 014 - i0 \cdot 0045) \\ &\simeq (0 \cdot 062 - i0 \cdot 032) \, \mathrm{m} \end{aligned}$$

where the time-variation term $\exp(i\omega t)$ has been omitted, as it is understood. The amplitude of pile-head displacement is

$$u_0(0) = [(0 \cdot 062)^2 + (0 \cdot 032)^2]^{1/2} \simeq 70 \ \mathrm{mm}$$

and the phase lag between pile-head deflexion and excitation is

$$\psi_u = \arctan\left(-\frac{0 \cdot 032}{0 \cdot 062}\right) \simeq -27 \cdot 2^\circ$$

For the pile-head rotation

$$\begin{aligned} \theta(0) &= \frac{100}{569 \times 0 \cdot 35^2} (0 \cdot 014 - i0 \cdot 0045) \\ &\quad + \frac{100}{569 \times 0 \cdot 35^3} (0 \cdot 003 - i0 \cdot 0005) \\ &\simeq 0 \cdot 032 - i0 \cdot 0085 \end{aligned}$$

The amplitude of rotation is

$$\begin{aligned} \theta_0(0) &= [(0 \cdot 032)^2 + (0 \cdot 0085)^2]^{1/2} \\ &\simeq 0 \cdot 033 \ \mathrm{rad} \simeq 1 \cdot 9^\circ \end{aligned}$$

and its phase lag from the excitation

$$\psi_\theta = \arctan\left(-\frac{0 \cdot 0085}{0 \cdot 032}\right) \simeq -14 \cdot 9^\circ$$

REFERENCES

Allen, N. F., Richart, F. E., Jr & Woods, R. D. (1980). Fluid wave propagation in saturated and nearly saturated sands. *J. Geotech. Engng Div. Am. Soc. Civ. Engrs* **106**, GT3, 235–254.

Angelides, D. C. & Roesset, J. M. (1981). Non-linear lateral dynamic stiffness of piles. *J. Geotech. Engng Div. Am. Soc. Civ. Engrs* **107**, GT11, 1443–1460.

Banerjee, P. K. & Davies, T. G. (1978). The behaviour of axially and laterally loaded single piles embedded in nonhomogeneous soils. *Géotechnique* **28**, No. 3, 309–326.

Blaney, G. W., Kausel, E. & Roesset, J. M. (1976). Dynamic stiffness of piles. *Proc. 2nd Int. Conf. Numer. Meth. Geomech., Blacksburg, Virginia.*

Dobry, R., Whitman, R. V. & Roesset, J. M. (1971). Soil properties and the one-dimensional theory of earthquake amplification. Research Report R71–18, Cambridge: Massachusetts Institute of Technology.

Dobry, R., Vicente, E., O'Rourke, M. J. & Roesset, J. M. (1982). Horizontal stiffness and damping of single piles. *J. Geotech. Engng Div. Am. Soc. Civ. Engrs* **108**, GT3, 439–459.

Gazetas, G. (1980). Static and dynamic displacements of foundations on heterogeneous multilayered soils. *Géotechnique* **30**, No. 2, 159–177.

Gazetas, G. (1981). Strip foundations on a cross-anisotropic soil layer subjected to dynamic loading. *Géotechnique* **31**, No. 2, 161–180.

Gazetas, G. (1983). Analysis of machine foundation vibrations: state of the art. *Int. J. Soil Dynam. & Earthq. Engng* **2**, No. 1, 1–42.

Gibson, R. E. (1967). Some results concerning displacements and stresses in a non-homogeneous elastic half-space. *Géotechnique* **17**, No. 1, 58–67.

Gibson, R. E. (1974). The analytical method in soil mechanics. *Géotechnique* **24**, No. 2, 115–140.

Harada, T., Kubo, K. & Katayama, T. (1981). *Dynamic soil–structure interaction by continuum formulation method.* Inst. Industrial Science, 29, No. 5. Tokyo: University of Tokyo.

Kagawa, T. & Kraft, L. M. (1980). Lateral load–deflection relationship of piles subjected to dynamic loadings. *Soils & Foundations* **20**, No. 4, 19–36.

Kagawa, T. & Kraft, L. M. (1981). Lateral pile response during earthquakes. *J. Geotech. Engng Div. Am. Soc. Civ. Engrs* **107**, GT12, 1713–1731.

Kausel, E. (1974). *Forced vibrations of circular foundations on layered media.* Research Report R74-11. Massachusetts: Massachusetts Institute of Technology.

Kausel, E., Roesset, J. M. & Waas, G. (1975). Dynamic analysis of footings on layered media. *J. Engng Mech. Div. Am. Soc. Civ. Engrs* **101**, EM5, 679–693.

Krishnan, R., Gazetas, G. & Velez, A. (1982). *Lateral response of free-head piles in nonhomogeneous soils.* Research Report CE82-07. New York: Rensselaer Polytechnic Institute.

Kuhlemeyer, R. L. (1979). Static and dynamic laterally loaded floating piles. *J. Geotech. Engng Div. Am. Soc. Civ. Engrs* **105**, GT2, 289–304.

Lamb, H. (1904). On the propagation of tremors over the surface of an elastic solid. *Phil Trans. Royal Soc.* **203**, 1–42.

Liou, D. D. & Penzien, J. (1977). *Seismic analysis of an offshore structure supported on pile foundations.* Report No. EERC77-25. Berkeley: University of California.

Matlock, H. (1970). Correlations for design of laterally loaded piles in soft clay. *Proc. 2nd Offshore Tech.*

Conf., Houston 1, 577–594.

Matlock, H. & Reese, L. C. (1960). Generalised solutions for laterally loaded piles. *J. Soil Mech. Fdns Div. Am. Soc. Civ. Engrs* **86**, SM5, 63–91.

Mindlin, R. D. (1936). Force at a point in the interior of a semi-infinite solid. *Physics* **7**, 195.

Nogami, T. & Novak, M. (1977). Resistance of soil to a horizontally vibrating pile. *Int. J. Earthq. Engng & Struct. Dyn.* **5**, 249–262.

Novak, M., Nogami, T. & Aboul-Ella, F. (1978). Dynamic soil reactions for plane strain case. *J. Engng Mech. Div. Am. Soc. Civ. Engrs* **104**, EM4, 953–959.

Novak, M. & Aboul-Ella, F. (1978). Impedance functions for piles in layered media. *J. Engng Mech. Div. Am. Soc. Civ. Engrs* **104**, EM6, 643–661.

Poulos, H. G. (1971a). Behaviour of laterally loaded piles: I—single piles. *J. Soil Mech. Fdns Div. Am. Soc. Civ. Engrs* **97**, SM5, 711–731.

Poulos, H. G. (1971b). Behaviour of laterally loaded piles: II—pile groups. *J. Soil Mech. Fdns Div. Am. Soc. Civ. Engrs* **97**, SM5, 733–751.

Poulos, H. G. (1973). Load–deflection prediction for laterally loaded piles. *Aust. Geomech. J.* G3, No. 1, 1–8.

Poulos, H. G & Davis, E. H. (1980). *Pile foundation analysis and design.* New York: Wiley.

Randolph, M. F. (1981). Response of flexible piles to lateral loading. *Géotechnique* **31**, No. 2, 247–259.

Tajimi, H. (1969). Dynamic analysis of a structure embedded in an elastic stratum. *Proc. 4th World Conf. Earthq. Engng, Chile.*

Wilson, E. L. (1965). Structural analysis of axisymmetric solids. *J. Am. Inst. Aer. Astr.* **3**, 2269–2274.

Wittke, W., et al. (1974). Bemessung von horizontal belastelen grassbohryahlen nach methode finites elemente. *Bauingenieur* **49**, 219–226.